Vegetation Greening Trends at Two Sites in the Canadian Arctic: 1984–2015

Authors: Edwards, Rebecca, and Treitz, Paul

AAAR

Vegetation greening trends at two sites in the Canadian Arctic: 1984–2015

Rebecca Edwards[1,2] and Paul Treitz[1,*]

[1]Department of Geography and Planning, Queen's University, Mackintosh-Corry Hall, Kingston, Ontario, K7L 3N6, Canada
[2]Ducks Unlimited Canada, 17504 111 Avenue NW, Edmonton, Alberta, T5S 1L6, Canada
[*]Corresponding author's email: paul.treitz@queensu.ca

ABSTRACT

This study examined vegetation greening at two arctic sites: the Apex River Watershed (ARW), Baffin Island, Nunavut (a Low Arctic site) and the Cape Bounty Arctic Watershed Observatory (CBAWO), Melville Island, Nunavut (a High Arctic site). The vegetation at both study sites was characterized using a supervised land-cover classification approach using high spatial resolution satellite remote sensing data (i.e., IKONOS [4 m] and WorldView-2 [2 m]). Meanwhile, Normalized Difference Vegetation Index (NDVI) data spanning the past 30 years were derived from intermediate spatial resolution data (i.e., Landsat TM/ETM/OLI [30 m]). The land-cover classifications were used to partition the Landsat NDVI time series by vegetation type. Climate variables (i.e., temperature, precipitation, and growing season length [GSL]) were examined to explore potential relationships of NDVI to climate warming trends. The results of the land-cover classifications demonstrated inherent trends of vegetation types along elevation and moisture gradients. The NDVI time series for the CBAWO (1985–2015) demonstrated an overall significant increase in greening, specifically in the dry and mesic vegetation types. Conversely, similar greening (overall or by vegetation type) was not observed for the ARW (1984–2015). Based on climate data from the nearest permanent weather station (Mould Bay, Nunavut), the overall increase in NDVI at the CBAWO was largely attributed to a significant increase in July temperatures and GSL.

INTRODUCTION

Global air surface temperatures have increased over the past several decades with the most rapid warming occurring in the Arctic (ACIA, 2004; Barber et al., 2008; AMAP, 2011; IPCC, 2013). Meanwhile, global circulation models (GCMs) estimate that arctic regions are likely to warm by several degrees over the next century (Huemmrich et al., 2010). These climatic changes in the Arctic will have notable, but variable impacts on tundra ecosystems; hence they are difficult to predict spatially and temporally. Impacts will include changes to sea ice cover, snow cover accumulation, hydrologic patterns, growing season length (GSL), permafrost (degradation/aggradation), vegetation productivity and biomass accumulation.

Individually, and in concert, these impacts will culminate in varied stresses to northern communities (ACIA, 2004, AMAP, 2011; IPCC, 2013; Abbott et al., 2016).

The satellite record has revealed that vegetation biomass and productivity in tundra ecosystems have already begun to change, resulting in a spatially variable trend of "Arctic greening" that is coincident with changes in surface temperatures (ACIA, 2004; Stow et al., 2004; Jia et al., 2009; Zeng et al., 2011; IPCC, 2013; Xu et al., 2013; Pearson et al., 2013; Fraser et al., 2011, 2014; Guay et al., 2014; Meyers-Smith et al., 2015; Moffat et al., 2016; Ju and Masek, 2016). For instance, the increase in vegetation productivity has been associated with an earlier onset of "green-up" and an extension of the growing season (i.e., phenological changes) (Walker et

al., 2006). The overall greening trend that has been observed over the satellite record has been supported by field experiments where warming simulations (Hollister et al., 2005; Walker et al., 2006; Elmendorf et al., 2012) and dendrochronology studies (Forbes et al., 2010; Myers-Smith et al., 2015) have been conducted. However, more recently, there is substantial evidence of "Arctic browning" in various regions of the circumpolar Arctic (Bjerke et al., 2014; Phoenix and Bjerke, 2016; Epstein et al., 2016), which has been attributed to an extended snow cover period (Bieniek et al., 2015) and reduced summer warmth index (SWI; sum of degree months above freezing) (Bhatt et al., 2013). Whether this is a temporary phenomenon, or an indication of a more systemic response to warming is yet to be determined (Phoenix and Bjerke, 2016).

Alterations to vegetation processes and structure that have been observed in the Low and High Arctic have been linked directly to climate warming (ACIA, 2004; Bhatt et al., 2013; IPCC, 2013; Tingley and Huybers, 2013). This increased warming will also drive other climate variables that will have an impact on vegetation change such as: (1) increased precipitation because of the early melt and loss of sea ice in the spring (Kattsov and Walsh, 2000; Gamon et al., 2013; Boisvert and Stroeve, 2015); (2) reduced snow cover in the spring as a result of early onset of snowmelt (i.e., longer growing season) (Hinzman et al., 2005; IPCC, 2013); (3) altered soil moisture conditions that are largely controlled by snow accumulation and drainage and linked to permafrost thaw (Hinzman et al., 2005; Collingwood et al., 2014); and (4) increased nutrient availability as a result of amplified leaf litter inputs (Welker et al., 2005).

Information derived from remote sensing data has greatly advanced our understanding of the Earth system, particularly with respect to vegetation processes. Remote sensing derivatives, such as the Normalized Difference Vegetation Index (NDVI) and time series satellite observations, have already provided evidence suggesting the Arctic is experiencing extended growing seasons and enhanced greening (Epstein et al., 2012; Bhatt et al., 2013; Gamon et al., 2013). NDVI is a remotely sensed measure of vegetation greenness related to the structural and physiological properties of the leaf, plant productivity, percent vegetation cover, and biomass (Laidler et al., 2008; Atkinson and Treitz, 2013; Forkel et al., 2013; Johansen and Tømmervik, 2014; Liu and Treitz, 2016). NDVI data are often used to analyze vegetation productivity and enable an efficient means for spatial and temporal comparisons using time series data (Brown et al., 2006; Yin et al., 2012). These data are now available at a range of spatial resolutions allowing researchers to examine vegetation patterns and processes from local to global scales.

There is a vast amount of literature across disciplines that reports on the application of satellite data for monitoring tundra environments. Coarse resolution NDVI time series data are widely used for regional to global vegetation monitoring because of their vast coverage of the Earth's surface at high temporal frequencies (Brown et al., 2006; Fensholt and Proud, 2012; Raynolds et al., 2012; Yin et al., 2012; Forkel et al., 2013; Guay et al., 2014; Epstein et al., 2016). These include several comprehensive studies that have applied AVHRR time series data to demonstrate notable decadal changes in vegetation greenness at northern high latitudes (Stow et al., 2003; Brown et al., 2006; Raynolds et al., 2012; Guay et al., 2014). Jia et al. (2003, 2009) used AVHRR data to investigate the interannual changes of vegetation greenness along latitudinal gradients in the Arctic (i.e., Alaska and Canada) to demonstrate how dominant vegetation types differ across bioclimatic zones. More recently, browning has been prevalent in the Arctic, particularly in Alaska (Epstein et al., 2015, 2016; Phoenix and Bjerke, 2016). Although allowing for repetitive synoptic coverage, AVHRR data are limited with respect to providing detailed information on vegetation structure, function, and type at local and watershed scales because of within-pixel heterogeneity of vegetation cover (Stow et al., 2004; Epstein et al., 2012).

To address this issue, intermediate resolution satellite data (e.g., Landsat TM/ETM/OLI) are now being used for more detailed vegetation analyses with a sufficient historical record to monitor change over time. Analyses over large areas using intermediate resolution satellite data in conjunction with ground studies have demonstrated that the homogeneous greening trend observed at coarse scales is quite heterogeneous at finer scales (Raynolds et al., 2013). Ju and Masek (2016) constructed a peak-summer Landsat composite of Canada and Alaska from 1984 to 2012 to compare to the Pinzon and Tucker (2014) GIMMS AVHRR NDVI3g data set. Based on the areal mean, their analyses revealed a 29.4% increase in greening and a 2.9% increase in browning, with the greening trend dominating browning for all cover types. Raynolds et al. (2013) conducted similar Landsat NDVI time series on the Foothills of the Alaska North Slope and found a 5% (statistically significant) increase in NDVI over a 22-year period.

Finally, researchers have developed linkages with above-ground biophysical variables for arctic vegetation types using high spatial resolution satellite data (e.g., IKONOS, GeoEye, WorldView-2) in conjunction with ground measurements, which can then be scaled-up to intermediate and regional scales (Stow et al., 2004; Epstein et al., 2012). Using high spatial resolution data for time series analysis is uncommon because of a short time

scale, yet these data can be used to supplement coarse resolution time series. For example, Urban et al. (2014) used coarse resolution GIMMS time series data (8 km resolution) to document greenness occurring in Pan-Arctic regions over the past 30 years, while using Landsat data (79 m resolution) and RapidEye data (5 m resolution) to measure woody vegetation cover and vegetation structure over a 40-year time span in local areas of Siberia. Moreover, the authors used different spatial and temporal scales to highlight the changes in land cover as a result of climate-induced trends in the past few decades.

Our study examined vegetation conditions over a 30-year time span at Low and High Arctic study sites located at the Apex River Watershed (ARW), Baffin Island, Nunavut (NU), and the Cape Bounty Arctic Watershed Observatory (CBAWO), Melville Island, NU, respectively. Intermediate (Landsat TM/ETM+/OLI) and high (WorldView-2 and IKONOS) spatial resolution remote sensing data were examined to determine if NDVI has changed during the period 1984 to 2015. To address this objective (1) vegetation types for each study site were classified using a supervised approach applied to Worldview-2 and IKONOS satellite data for the ARW and CBAWO respectively; (2) NDVI time series were derived using Landsat data for both study sites (i.e., 1984 to 2015 for the ARW; 1985 to 2015 for the CBAWO) and coupled with high spatial resolution land-cover classifications to identify change associated with specific vegetation types; and (3) climate variables (temperature, precipitation, and GSL) were analyzed to determine if changes in NDVI could be directly linked to trends in these climate variables.

STUDY SITES

This study was conducted at two study sites in the Low and High Arctic: i.e., the ARW, Baffin Island, NU, and the CBAWO, Melville Island, NU, respectively (Fig. 1).

Apex River Watershed, Baffin Island, NU

The ARW (63°48′N, 68°31′W) is 58 km² and is characterized by undulating topography ranging from approximately 50 to 300 m above sea level, with the highest elevation located in the northern reaches of the watershed. The ARW consists of sand and gravel glaciofluvial and glaciomarine sediment, which is underlain by Ordovician sedimentary rocks and Precambrian granite-gneiss bedrock (Jacobs et al., 1997; Natural Resources Canada, 2012, 2015). The mean monthly air temperatures in Iqaluit range from 8.2 °C in July to −26.9 °C in January with an annual mean of −9.3 °C, giving rise to a relatively short snow-free period

and hence a short growing season (Leblanc et al., 2012). The total annual precipitation, predominantly falling as snow, averages 412 mm (Environment and Climate Change Canada, 2015). The ARW is underlain by continuous permafrost, giving rise to an active layer ranging from 0.5 to 2.0 m depending on the drainage and substrate materials (Jacobs et al., 1997; Leblanc et al., 2012). The average growing season starts in June and ends in August with peak growing conditions occurring in late July (Environment and Climate Change Canada, 2015). According to the Circumpolar Arctic Vegetation Map (CAVM), the ARW is located in Bioclimatic Zone D, yet also contains hemi-prostrate dwarf shrub, which is more common in Subzone C (CAVM Team, 2003; Walker et al., 2005). Five broad vegetation types have been described for the ARW: (1) dry vegetation type (P1)—prostrate dwarf shrub, herb tundra; (2) mesic vegetation type (P2)—prostrate/hemi-prostrate, dwarf shrub tundra; (3) mesic vegetation type (G2)—graminoid, prostrate dwarf shrub; (4) mesic vegetation type (G3)—non-tussock sedge, dwarf shrub, moss tundra; and (5) wet vegetation type (W1)—sedge/grass, moss wetlands (Obradovic and Sklash, 1986; Jacobs et al., 1997; CAVM Team, 2003; Walker et al., 2005).

Cape Bounty Arctic Watershed Observatory, Melville Island, NU

The CBAWO (74°55′N, 109°35′W) consists of two adjacent watersheds spanning 30 km² exhibiting topographic relief that ranges from 5 to 125 m above sea level. The most common surficial material is weathered bedrock predominantly where linear bands of the Devonian formation and the sediments of the Sverdrup basin are clearly delineated (Edlund, 1993). The site is overlain by glacial till (i.e., Winter Harbour Till) and a thick carbonate-rich till with crystalline clasts draped over the sedimentary bedrock (Edlund, 1993). The mean July temperature and precipitation derived from data collected at the Main Meteorological Station at the CBAWO from 2003 to 2015 is 6.2 °C and 31 mm, respectively (Lamoureux, 2015). The CBAWO is in a continuous permafrost region with an active layer depth of approximately 0.5–1.0 m (Atkinson and Treitz, 2013). The melt season extends from June through August, which limits the short growing season from late June to early August (Environment and Climate Change Canada, 2015). The CBAWO falls within Bioclimatic Subzone B (CAVM Team, 2003; Walker et al., 2005). At the scale of the Circumpolar Arctic Vegetation Map, the vegetation at the CBAWO is classified as G2—graminoid, prostrate dwarf-shrub, forb tundra (CAVM Team, 2003). At the local scale, the vegetation is heterogeneous and varies with drainage. A supervised land cover classification for the CBAWO
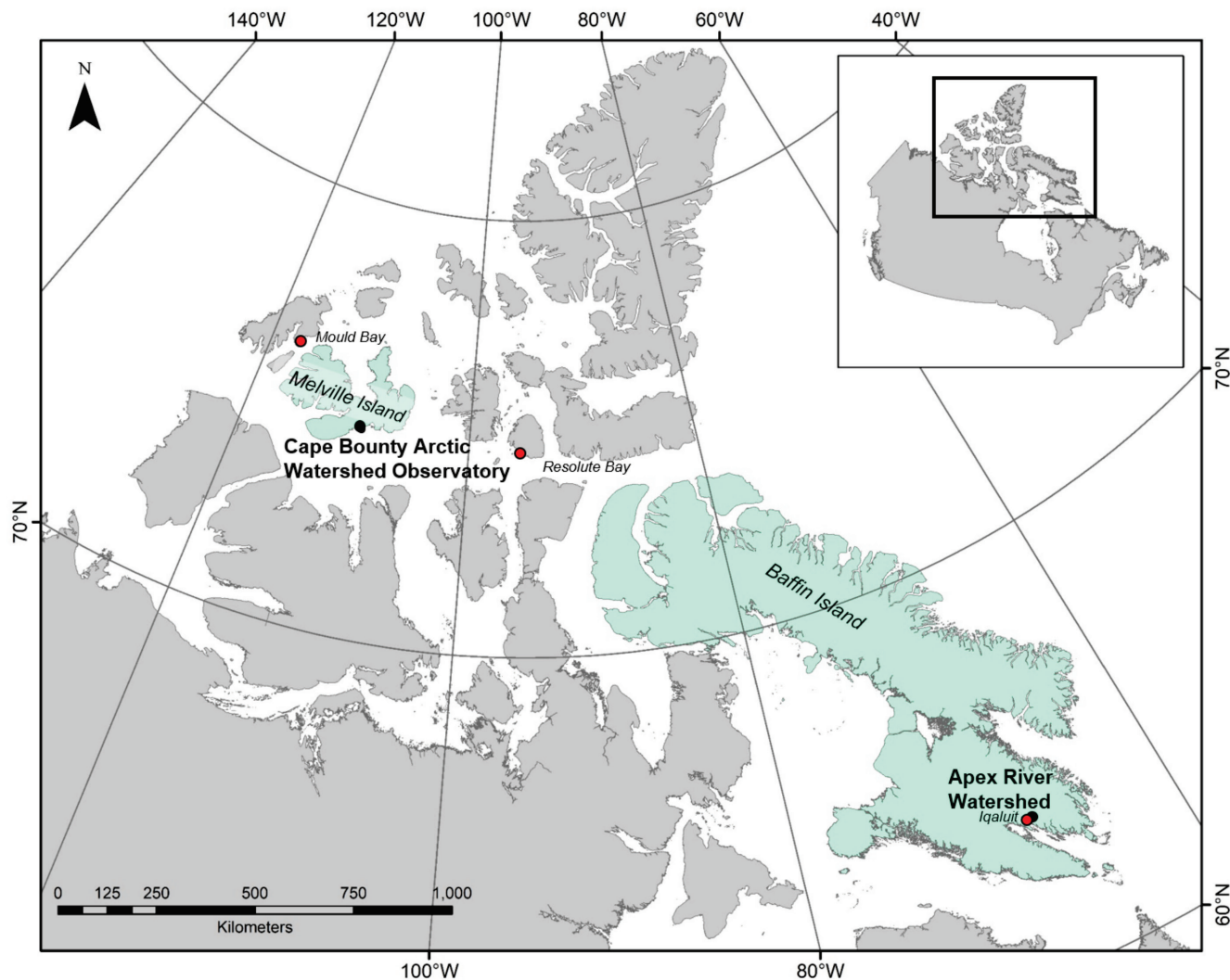
FIGURE 1.   Study locations on Melville Island (Cape Bounty Arctic Watershed Observatory—CBAWO) and Baffin Island (Apex River Watershed—ARW), Nunavut, Canada. Climate data were obtained from climate stations at Mould Bay and Iqaluit for the CBAWO and ARW, respectively. Resolute Bay climate station is included for reference.

was completed by Gregory (2011) based on field data collected in 2008 and 2009 and high spatial resolution (4 m) IKONOS data collected on 22 July 2008 (overall classification accuracy = 83%; Kappa = 0.79). Three vegetation types, closely related to distinctive moisture regimes (i.e., along a moisture gradient) were classified: polar semi-desert, mesic tundra, and wet sedge meadows (Gregory, 2011; Atkinson and Treitz, 2012) (Fig. 2).

METHODS

Data Collection

Field sampling was carried out in the ARW from 20 June to 10 August 2015 (i.e., during the growing season) using methods developed for the international tundra experiment (ITEX) (Molau and Mølgaard, 1996).

The sampling procedure was designed to collect in situ percent vegetation cover (PVC) measurements by functional group (i.e., shrubs, graminoids/sedges, mosses, forbs, and lichens) to characterize the vegetation types in the ARW for the land-cover classification. Two transects were sampled at each of seven sites (i.e., for a total of 14 transects) (Fig. 3). Each transect was 100 m in length and oriented across different slope angles to ensure that sufficient data were collected to acquire a representative sample of the vegetation types (and environmental conditions) present in the study site (i.e., vegetation variability across the terrain [elevation, slope, aspect] and moisture regimes). Vegetation data were collected in 6 m × 6 m plots located at 20 m intervals along each transect. Each 6 m × 6 m plot was divided into four sections (i.e., 3 m × 3 m quadrants) and the center of each quadrant was sampled with a 0.6 m × 0.6 m quadrat (Fig. 3).
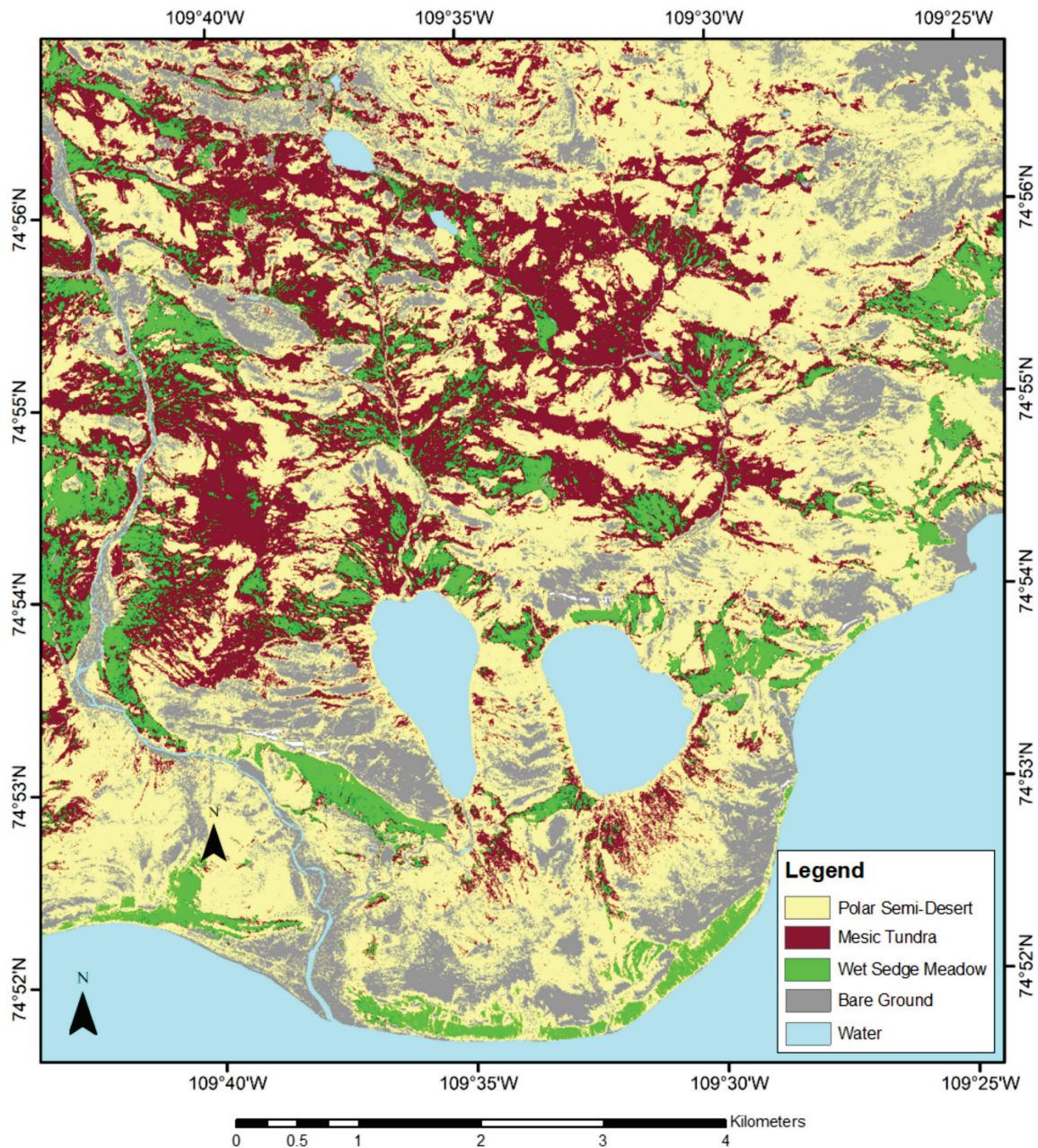
FIGURE 2. Vegetation classification of the CBAWO. This classification was derived from IKONOS high spatial resolution data acquired on 4 July 2008 using a supervised approach (Gregory, 2011).

The plots at each transect location were georeferenced and utilized as calibration and validation data for the vegetation classification. The sampling procedure (i.e., plots, quadrants, and quadrats) was designed so that field data could be related to the spatial resolution of World-View–2 (~2 m) while being able to "scale up" to a 30 m Landsat pixel used in the NDVI time series analyses. Additional vegetation sites were established approximately every 30 m along routes connecting transect locations to enhance the sample size for image classification (i.e.,

calibration and validation). Global Positioning System (GPS) coordinates and vegetation descriptions were recorded with representative digital photographs to categorize vegetation types at these locations.

Satellite Image Processing

High spatial resolution satellite multispectral data (i.e., WorldView–2) were used in this study to establish a vegetation classification for the ARW (Table
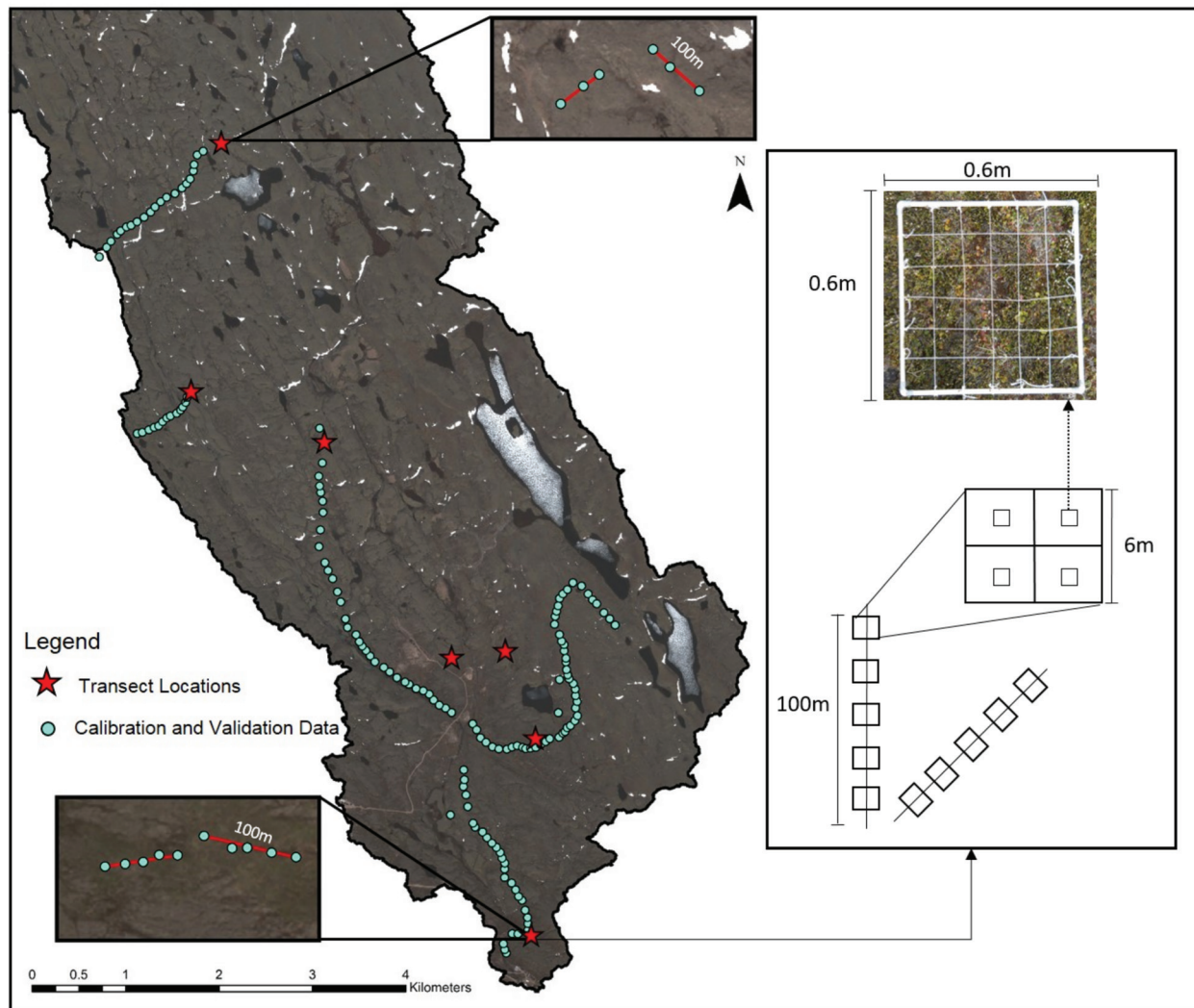
FIGURE 3. Sampling design for the Apex River Watershed (ARW). At seven sample sites, two 100-m transects were sampled using 6 m × 6 m plots. At each plot, the center of each quadrant (3 m × 3 m) was sampled with a 0.6 m × 0.6 m quadrat to estimate percent vegetation cover (PVC). The number and orientation of transects varied at each location in order to sample across environmental and topographic gradients. Right inset—examples of the 0.6 m × 0.6 m quadrats within each plot to determine PVC using the ITEX method. Additional calibration and validation data for image classification were collected while traveling from one transect location to another.

1). The WorldView-2 data (8 spectral channels with a spatial resolution of ~2 m) were collected at peak growing season on 21 July 2015. The digital numbers (DN) were converted to top of atmosphere (TOA) reflectance using the TOA radiometric correction in the ENVI Image Analysis Software (v. 5.2). The land-cover classification for the ARW was subsequently used to examine the overall greenness by vegetation type over time using intermediate scale remote sensing data (i.e., NDVI data derived from Landsat). Similarly, the classification for the CBAWO generated by Gregory (2011) was used to generate the Landsat NDVI time series by vegetation type. In this sense, both classifications were used to segment the study sites into vegetation types, for which NDVI time series were generated for each vegetation type and for the watersheds overall.

For the NDVI time series analyses, cloud-free Landsat TM/ETM/OLI data were collected during the growing season (i.e., between 10 July and 15 August) for the ARW and CBAWO (Table 1). The orthorectified Landsat data (30 m spatial resolution) were downloaded from the U.S. Geological Survey GLOVIS website (USGS, 2015). The red and near-infrared bands were extracted from each image to derive NDVI for each date. The Landsat data were radiometrically normalized to compensate for atmospheric path radiance and errors associated with the

TABLE 1

Satellite image data used for vegetation analyses for the ARW and the CBAWO. The asterisk (*) represents dates that could potentially be anomalies within the NDVI time series satellite data (i.e., early or late in the growing season).

	Path/Row	Satellite	Year	Date
High-Resolution Scenes				
LT50180151985199PAC00	018/015	WorldView-2	2015	Jul-20
LT50170151989203PAC00	017/015	IKONOS	2008	Jul-22
Landsat Scenes—ARW				
LT50180151985199PAC00	018/015	Landsat 5 TM	1984	Jul-18
LT50170151989203PAC00	017/015	Landsat 5 TM	1989	Jul-22
LT50180151991216PAC00	018/015	Landsat 5 TM	1991	Aug-04
LT50170152004213GNC00	017/015	Landsat 5 TM	2004	Jul-31
LT50170152008208GNC00	017/015	Landsat 5 TM	2008	Jul-26
LT50180152010188GNC00	018/015	Landsat 5 TM	2011	Jul-10*
LC80180152015218LGN00	018/015	Landsat 8 OLI	2015	Aug-06
Landsat Scenes—CBAWO				
LT50560071985193PAC00	056/007	Landsat 5 TM	1985	Jul-12
LT50550071988195PAC00	055/007	Landsat 5 TM	1988	Jul-13
LT50550071994195PAC00	055/007	Landsat 5 TM	1994	Jul-14
LT50550071999225PAC00	055/007	Landsat 5 TM	1999	Aug-14*
LT50530072006214PAC02	053/007	Landsat 5 TM	2006	Aug-02
LT50540072009213PAC01	054/007	Landsat 5 TM	2009	Aug-01
LC80540072015198LGN00	054/007	Landsat 8 OLI	2015	Jul-17

use of multiple sensors and images collected at different dates using pseudo-invariant features (PIFs) and regression (Jensen, 2005). This method involves selecting similar PIFs in each image that do not change spectrally over time in order to correct for brightness variations that are related to different atmospheric conditions (Jensen, 2005). First, a cloud-free image was selected as a base image for the time series. Approximately 10–20 dark- and light-colored PIFs (i.e., sandbanks, bedrock, deep water, etc.) were selected in the images by using the region-of-interest (ROI) tool. ROI statistics were extracted from each PIF, and the average reflectance values were recorded. Regression analyses for each band were used to determine the relationship between the spectral characteristics of the PIFs from each image in the time series to the PIFs of the base image (Jensen, 2005). After the image data were normalized, NDVI data were derived using the band math function. The satellite data were masked to include the watershed and exclude roads, rivers, and lakes (Natural Resources Canada, 2015). Additionally, areas of cloud and cloud shadow were manually masked by analyzing large differences in NDVI between scenes.

Land-Cover Classification

The land-cover classifications for the ARW and the CBAWO are important in this study to determine if different vegetation types at each site have experienced change over time, and if so, at what rates. It is anticipated that vegetation types defined along a moisture gradient at these sites have responded or will respond differently to changes in climate. The classification procedure for the ARW began by classifying the World-View-2 imagery employing a supervised approach with the Support Vector Machine (SVM) algorithm to distinguish five spectral classes using the CAVM as a guide. Initially, the calibration locations were separated into five vegetation classes and two non-vegetated classes. However, analysis of the spectral data revealed that only three vegetated and two non-vegetated classes were spectrally separable (i.e., the mesic sites were collapsed into a single mesic site and the non-vegetated classes were combined into a single class of bare ground). The land-cover classification was calibrated using 115 sample sites (total = 923 calibration pixels; 78 dry tundra, 408 mesic tundra, 66 wet tundra, 371 bare ground). Validation of the classification was based

on 67 sample sites (total = 596 validation pixels; 99 dry tundra, 324 mesic tundra, 46 wet tundra, 127 bare ground). Binomial probability theory was used to determine a suitable sample size for validation (i.e., expected map accuracy = 85%; allowable error = 10%; minimum sample size = 51) (Fitzpatrick-Lins, 1981).

NDVI Time Series Analysis

Pixels were randomly selected for each Landsat time series image (1984–2015 for the ARW and 1985–2015 for the CBAWO) based on the vegetation types in the WorldView-2 and IKONOS vegetation classifications; specifically, where there were large homogeneous areas that would be representative for Landsat pixels (i.e., 30 m). Approximately 100 NDVI pixels were selected from each vegetation type for each of the two study sites. A cluster-sampling scheme was adopted because most of the pixels in the Landsat data were in large homogeneous areas. Clustered samples did not exceed 10 pixels for any given sample site in order to minimize bias associated with spatial autocorrelation (Jensen, 2005). Hence, a minimum of 10 independent sample sites (with up to 10 pixels per site) were randomly selected for a total of 100 NDVI pixels per vegetation type. First, the average NDVI values (i.e., of all sample pixels) for each Landsat time series were extracted to determine the overall trend in NDVI for each study site. Second, in order to examine any differences in vegetation growth by vegetation type, the average NDVI values were extracted and averaged for each vegetation type by year.

Climate Variables—Temperature, Precipitation and Growing Season Length

Mean July homogenized temperature (1946–2015) and precipitation (1946–2007) data were acquired from the Environment and Climate Change Canada (2015) archive for the Iqaluit weather station. Similarly, mean July homogenized temperature (1948–2015) and precipitation (1948–2007) data were acquired for Mould Bay (the nearest permanent weather station ~300 km west of the CBAWO). Anomalies were measured as the residual variations in climate variables to reduce the systematic effect of seasonality over a long-time series (i.e., base periods of 1971–2000 and 1961–1990 for temperature and precipitation, respectively) (Olthof and Latifovic, 2007; Tingley and Huybers, 2013).

The monthly mean daily minimum and maximum temperatures from 1946 to 2015 for Iqaluit and 1948 to 2015 for Mould Bay were also acquired from Environ-

ment and Climate Change Canada (2015). The growing degree days (GDD) were calculated as the cumulative daily mean temperature above a selected threshold temperature (i.e., in the Arctic the threshold temperature for GDD is 5 °C). The GDD was calculated from the equation below for each study site:

$$GDD= [(T_{max} + T_{min})/2] - T_{base} \qquad (1)$$

where T_{max} and T_{min} are the daily maximum and minimum temperatures and T_{base} is 5 °C (GDD is unitless). The GSL was calculated by summing the number of days for which the average temperature exceeded the threshold (5 °C) over the growing season from June to August (Carter, 1998; Førland et al., 2004; Skaugen and Tveito, 2004; Weijers et al., 2013).

Results

Land-Cover Classification

The supervised classification for the ARW generated a single non-vegetated class and three vegetated classes: (1) bare ground; (2) polar semi-desert (prostrate dwarf shrub/herb tundra); (3) mesic tundra (hemiprostrate/graminoid prostrate dwarf shrub); and (4) wet sedge meadow (sedge/grass moss wetlands) (Fig. 4). The overall classification accuracy was 73.2% (Kappa = 0.53). Mesic tundra dominates the landscape (51.6%) followed by polar semi-desert (27.6 %), bare ground (12.3%), and wet sedge meadow (8.6%).

NDVI Time Series Analysis

The average NDVI for the ARW over the period of 1984–2015 indicates an overall increasing trend for the watershed, yet this trend is not statistically significant (Table 2; Fig. 5, part a). This trend is driven largely by a slightly increasing trend for the mesic tundra of 0.38% yr^{-1}, albeit not significant. Therefore, there is no distinct change in NDVI at the ARW site over the period 1984–2015. Analyzing the NDVI patterns for each vegetation type illustrates similar increasing trends from 1984 to 2015 with decreases from 2008 to 2011 followed by an increase from 2011 to 2015 (Fig. 5, part a). It is important to note that the 2011 NDVI data for the ARW were acquired early in the growing season (i.e., 10 July) and appear somewhat anomalous, particularly for the wet sedge meadow (Fig. 5, part a).

In contrast, the average NDVI for the CBAWO indicates a significant positive trend from 1985 to 2015
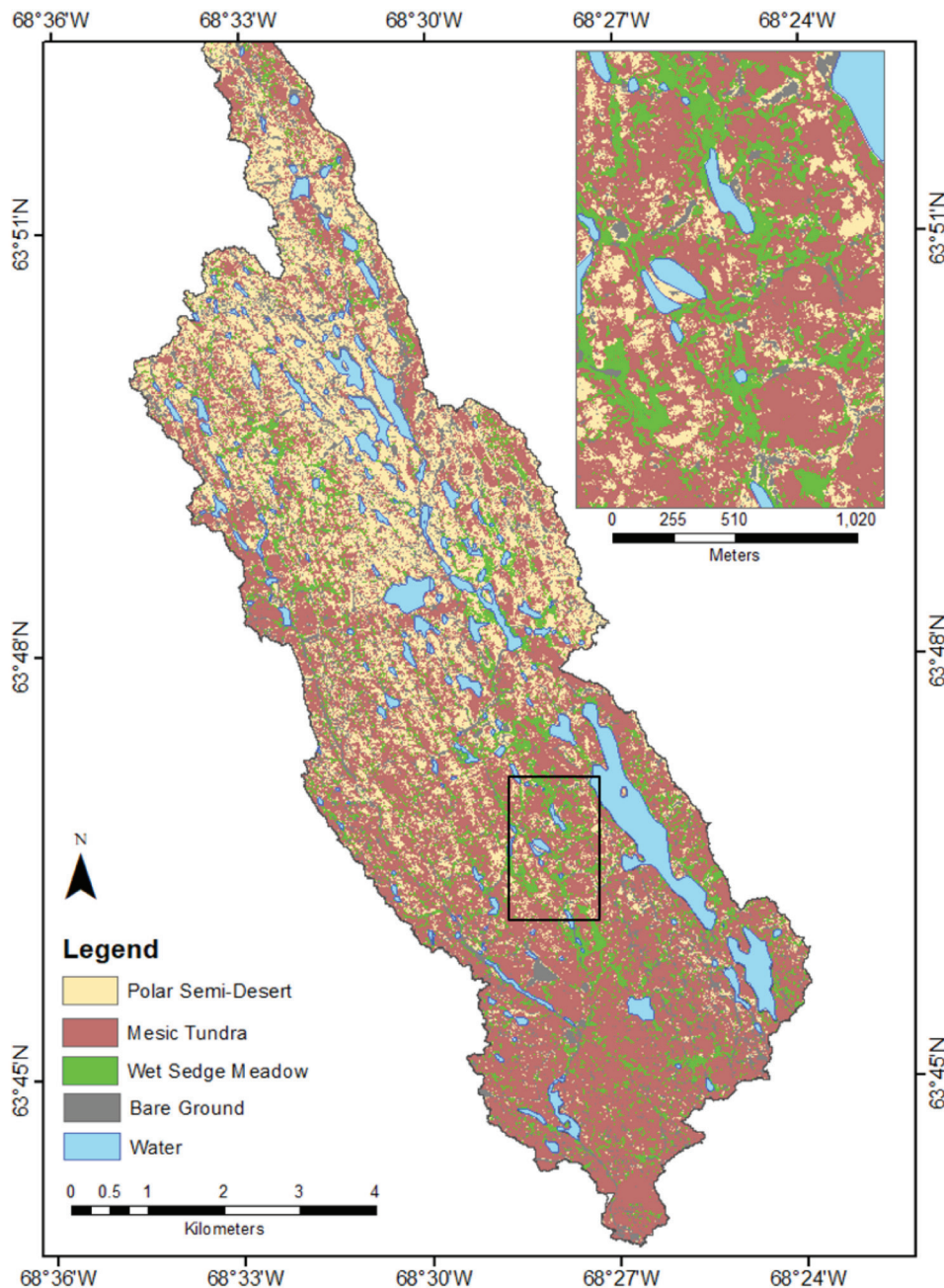
FIGURE 4. Supervised land-cover classification for the ARW using high resolution WorldView-2 data. The inset provides a more detailed depiction of the vegetation classes at a larger scale.

for the entire watershed (Table 2; Fig. 5, part b). This overall trend results from significant positive trends in NDVI for the mesic tundra and polar semi-desert with increases of 1.3% yr^{-1} and 0.82% yr^{-1}, respectively, and a non-significant trend for wet sedge meadow (i.e., an increase of 0.19% yr^{-1}). NDVI patterns for each vegetation type show similar increasing trends from 1985 to 2015 with sharp decreases from 1988 to 1999. Again, it should be noted that the 1999 NDVI data for the CBAWO (which divert from the trend) were acquired late in the growing season (i.e., 14 August) and may have been impacted by cooler temperatures or even the onset of freeze-up (Fig. 5, part b).

Climate Variables—Temperature, Precipitation, and Growing Season Length

The results from the NDVI time series indicate an increase in greenness at the High Arctic site (CBAWO) compared to the Low Arctic site (ARW), particularly for the mesic tundra and polar semi-desert. Here, temperature, precipitation, and GSL are examined as potential controls on the NDVI trends observed at these sites. The mean homogenized July temperature and precipitation anomalies for Iqaluit demonstrate variability over the past 60 years with no significant

TABLE 2

Linear regression results for the NDVI time series analysis. Significant trends in bold.

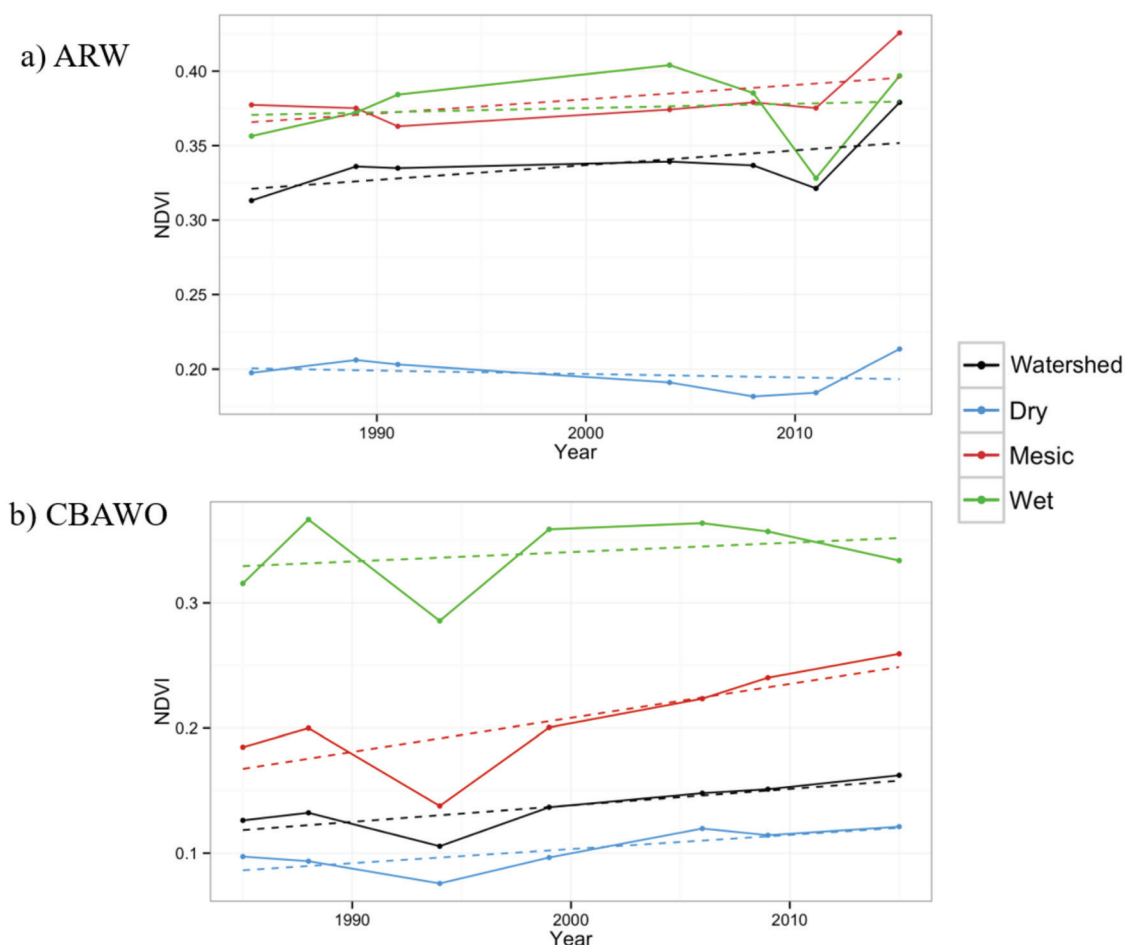| Sites	Vegetation type	Equation	ADJ R^2	P-value (<0.05)
ARW		$0.0031x - 5.8221$	0.20	0.170
	Polar semi–desert	$-0.006x + 0.1992$	0.01	0.607
	Mesic tundra	$0.0058x + 0.3583$	0.38	0.176
	Wet sedge meadow	$0.0012x + 0.3704$	0.01	0.773
CBAWO		$0.0013x - 2.4972$	0.54	0.040
	Polar semi–desert	$0.0011x - 2.1598$	0.49	**0.046**
	Mesic tundra	$0.0027x - 5.2027$	0.49	**0.048**
	Wet Sedge Meadow	$0.0008x - 1.162$	−0.10	0.549

FIGURE 5. **(a) NDVI time series by vegetation type in the ARW (1984–2015). The ARW represented in black contains all the usable pixels located in the watershed. (b) NDVI time series by vegetation type in the CBAWO (1985–2015). The CBAWO represented in black contains all the usable pixels located in the watershed.**

trends (Table 3; Fig. 6, parts a and c). Even after removing the 2015 data point (i.e., an anomaly in the temperature trend) there was no significant trend in temperature over the period studied. However, the mean homogenized July temperature for Mould Bay indicates a significant positive trend over the past 60 years (Table 3; Fig. 6, part b). Meanwhile, the homogenized precipitation illustrates the natural variability in the Mould Bay data (with no clear trend) (Table 3; Fig. 6, part d).

TABLE 3

Linear regression results for temperature, precipitation, and GSL time series analysis. Significant trends in bold.

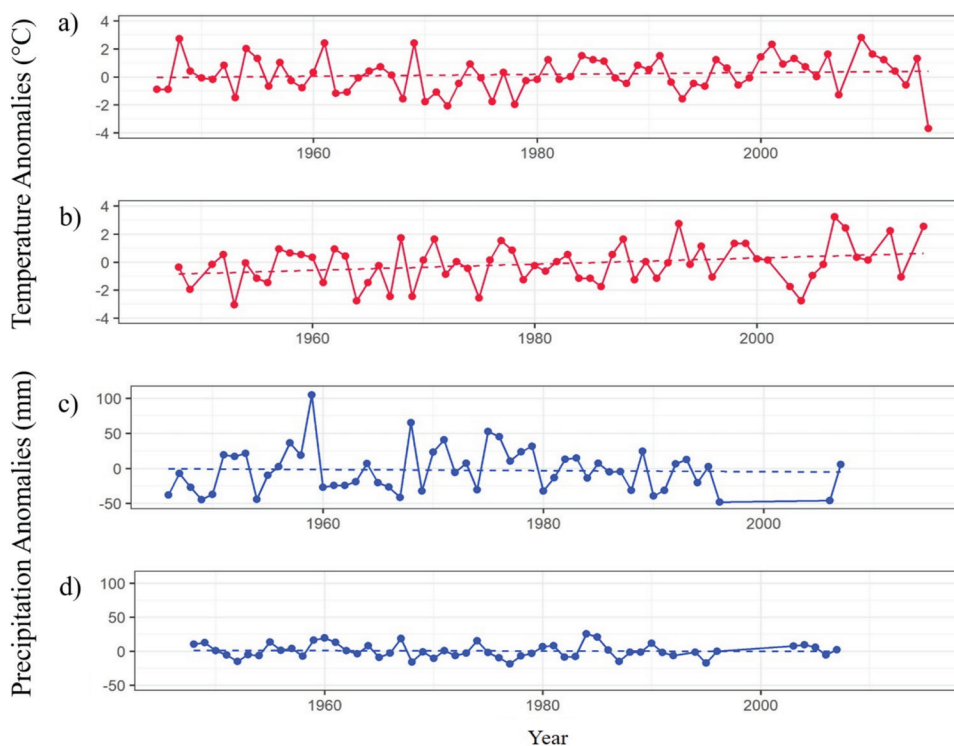| Sites	Climate Variables	Equation	ADJ R^2	P-value (<0.05)
ARW	Temperature	$0.0065x - 12.653$	-0.004	0.40 ($n = 69$)
	Precipitation	$-0.075x + 145.29$	-0.018	0.79 ($n = 53$)
	GSL	$0.0807x - 102.47$	0.013	0.17 ($n = 70$)
Mould Bay	Temperature	$0.0223x - 44.214$	0.070	**0.02 ($n = 63$)**
	Precipitation	$-0.0300x + 59.77$	-0.017	0.73 ($n = 52$)
	GSL	$0.1488x - 279.35$	0.076	**0.02 ($n = 66$)**

FIGURE 6. (a) Iqaluit homogenized mean July temperature anomalies from 1946 to 2014 (base period 1971–2000) supplemented with the 2015 July monthly temperature anomaly (missing data: 2008); (b) Mould Bay homogenized mean July temperature anomalies from 1948 to 2015 (base period 1971–2000) (missing data for Mould Bay: 1950, 1997, 2002, 2011, 2014); (c) Iqaluit homogenized total July precipitation from 1946 to 2007 (base period 1961–1990) (missing data: 1997–2005); (d) Mould Bay homogenized total July precipitation from 1948 to 2007 (base period 1961–1990) (missing data for Mould Bay: 1993, 1997–2002) (Environment and Climate Change Canada, 2015).

The results for GSL for Iqaluit show a slightly increasing trend from 1946 to 2015, albeit not significant (Table 3; Fig. 7, part a). In 2015, there was a large anomaly in the data set, with only 26 GDD, whereas the average throughout the time series is approximately 63 days. It is important to note that if the 2015 data were to be removed, the results would still not indicate a significant positive trend. Conversely, there is an increasing positive trend in GSL at Mould Bay from 1948 to 2015 (Fig. 7, part b).

Discussion

Land-Cover Classification

The classification of high spatial resolution remote sensing data was used to segment the study sites into general vegetation types defined along a soil moisture gradient (polar semi-desert, mesic tundra, wet sedge meadow). At the ARW, there is an inherent trend in vegetation types defined by topography, where denser,
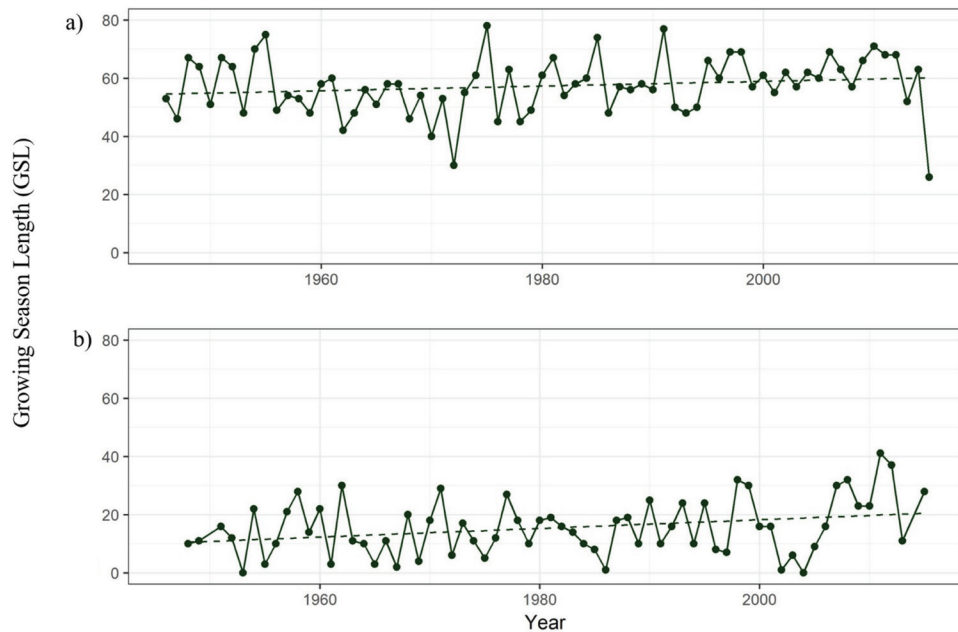
FIGURE 7. (a) Growing season length from 1946 to 2015 calculated from the minimum and maximum mean daily temperature for Iqaluit A and Iqaluit UA weather stations; (b) growing season length from 1948 to 2015 calculated from the minimum and maximum mean daily temperature for Mould Bay A and Mould Bay CS weather stations (missing data for Mould Bay: 1950, 2014) (Environment and Climate Change Canada, 2015).

lusher vegetation tends to be near and just above sea level in the south, whereas sparse and barren vegetation tends to be predominant in the north at higher elevations (Fig. 4). In the southern portion of the watershed, dense vegetation, including shrub, sedge, and forb functional groups, tends to be found along streams, rivers, and lakes, and in concavities or microtopographic depressions. Conversely, in the northern portion of the watershed, rock and thin soils with small patchy shrub and forb species tend to dominate. Topography is the primary control over seasonal soil moisture and is the reason wet vegetation inhabits low-lying areas near permanent snow packs, deep depressions, and areas in close proximity to lakes and rivers. On the other hand, dry vegetation inhabits well-drained areas such as the tops of hills, shallow soils, and exposed areas. Hence, vegetation types, and their spectral response, are largely related to soil moisture (Ostendorf and Reynolds, 1998; Necsoiu et al., 2013; Collingwood et al., 2014). This relationship, that is, the interdependence between terrain, moisture regime, and vegetation type, is also evident at the CBAWO. More broadly, it follows that vegetation types will vary spatially across the Arctic based on moisture availability throughout the growing season, a condition that is susceptible to changes in climate and permafrost condition. Hence, vegetation condition (i.e., NDVI) is a strong surrogate for persistent seasonal moisture regime at high latitudes. In this study we assumed that vegetation types did not change over the time period studied. However, given the warming observed at high latitudes, it seems reasonable to expect productivity of vegetation types to increase (or decrease) over a 30-year time frame.

Also, it can be expected that vegetation type boundaries will change over the long term in concert with continued warming (or cooling), changes in moisture regime, and permafrost condition. Hence, classification of vegetation types over longer time periods may provide additional evidence of changes in ecosystem structure and function as longer time series of intermediate and high spatial resolution remote sensing data accumulate.

These terrain and environmental factors control where certain vegetation types reside, giving rise to heterogeneous vegetation types across fine spatial scales. High spatial resolution data are useful for characterizing the fine-scale variability of vegetation signatures, discriminating vegetation type boundaries, identifying areas of disturbance, and enhancing our ability to scale synoptic predictions (Thomas et al., 2002; Stow et al., 2004; Rudy et al., 2013; Cameron and Lantz, 2016; Davidson et al., 2016). While pixel-based classifications have exhibited accurate results in arctic vegetation classifications (Gregory, 2011; Atkinson and Treitz, 2012; Olthof and Fraser, 2014), the classification accuracy for the ARW was moderate. This may be attributed to a more complex terrain (i.e., moisture conditions) and more diverse and abundant vegetation present in the ARW, at least in comparison to the CBAWO. Given the high spatial variability of vegetation types, PVC, and soil moisture in the ARW (i.e., various mixtures of vascular plants, bryophytes, and bare soil and till), relying solely on visible and near-infrared spectral signatures to classify vegetation types using high spatial resolution data may not be sufficiently accurate or precise, particularly when attempting to partition vegeta-

tion types along a continuous moisture gradient. New satellites (e.g., WorldView-3) provide high spatial and spectral resolution data that extend through the short-wave infrared (SWIR) and are capable of collecting data in stereo for the derivation of precise digital elevation models (DEMs). These additional data should improve our capacity for classifying vegetation types in the Arctic that are closely related to moisture regime (Bratsch et al., 2016). In addition, the application of other classification methods such as object-based and neural network classifiers may be more applicable to this environment (Chen et al., 2010; Lantz et al., 2010; Collingwood et al., 2014), particularly given their capacity for incorporating additional contextual variables into the classification (e.g., elevation, slope, aspect, texture, wetness, etc.) to further refine the classification of vegetation types (Lantz et al., 2010). It should be noted that these types of studies require field campaigns to calibrate and validate remote sensing data analyses, regardless of the scale of observation (Guay et al., 2014).

NDVI Time Series Analysis

The mesic tundra and polar semi–desert for the ARW have higher NDVI values than the CBAWO, whereas the wet sedge meadows exhibit similar NDVI values (Fig. 5). This is not surprising given the overall warmer climate in the Low Arctic, which gives rise to higher biodiversity and productivity (Ju and Masek, 2016). The mesic tundra demonstrates different NDVI values between sites. This can likely be attributed to the mesic tundra at the ARW having greater biodiversity and biomass as a result of the inclusion of more vascular plants, including erect, woody shrubs (i.e., *Salix* spp.; *Dryas octopetala, Cassiope tetragona, Empetrum* spp.) than are present at the CBAWO (Hope et al., 1993; Jacobs et al., 1997; Atkinson and Treitz, 2012; Liu and Treitz, 2016). Also, for the polar semi–desert, the ARW exhibits slightly higher NDVI values than those at the CBAWO (Fig. 5). The polar semi–desert at the CBAWO exhibits higher proportions of exposed soil in its polygon structure than those at the ARW. Polar semi–deserts vary across latitudes in that the proportion of exposed soil within this vegetation type tends to increase with latitude as vegetation becomes more sporadic and restricted to small depressions of ice–wedge polygons (Atkinson and Treitz, 2012, 2013; Liu and Treitz, 2016).

In general, studies based on satellite observations have reported an increase in NDVI (i.e., shrub expansion and/or vegetation growth) across the Arctic at coarse (Jia and Epstein, 2003; Guay et al., 2014; Epstein et al., 2012, 2016) and intermediate scales (Fraser et al., 2011; Ju and Masek, 2016). Although greening trends tend to be predominant across the Arctic, the rates of greening vary significantly over space and time with some areas exhibiting browning, an outcome that is relatively recent and not well understood (Beck and Goetz, 2011; Guay et al., 2014). It is clear that the productivity of vegetation types across the Arctic (i.e., based on NDVI) is spatially and temporally variable as a result of similar variability of environmental drivers.

Epstein et al. (2012) found an increase in aboveground phytomass across the circumpolar arctic tundra in the past three decades using NDVI derived from AVHRR data. The authors determined that the greatest increases in phytomass occurred in the southernmost tundra subzones (C–E), albeit there was a high degree of heterogeneity across vegetation types. Alternatively, in the context of specific bioclimatic subzones and vegetation communities, Jia et al. (2009) found a greater increase in peak NDVI in the High Arctic (0.49–0.79% yr^{-1}; dominated by prostrate dwarf shrubs, mosses, and lichens) compared to the Low Arctic (0.46–0.69% yr^{-1}; dominated by erect dwarf shrubs and graminoids) for the period 1982–2006. The authors suggested this contrast is likely because of different time series examined, indicating a non-linear response of arctic vegetation types to warming and/or cooling trends. For instance, it has been observed that a period of greening can be followed by a period of browning (Epstein et al., 2015). Meanwhile, based on Moderate Resolution Imaging Spectroradiometer (MODIS) data analysis, Miles and Esau (2016) reported relatively equal proportions of greening (8.4%) and browning (9.6%) for a study site in northern west Siberia, with a general consensus that greening tends to be associated with tundra ecosystems and browning with the boreal forest, an observation consistent with other studies (Walker et al., 2009; Epstein et al., 2016). This variable ecosystem response has been linked to temperature and cloudiness by Seddon et al. (2016) based on their analysis of MODIS data over a 14-year period.

In this study, Landsat data, coupled with high spatial resolution land-cover classifications, were useful in identifying greenness occurring at landscape scales by vegetation type. The Landsat time series analysis revealed an overall increase in NDVI at the CBAWO at the western extent of the Canadian High Arctic (specifically for the dry and mesic vegetation types) (Table 2; Fig. 5). Meanwhile, no significant change in NDVI was observed for the ARW located at the eastern extent of the Canadian Low Arctic (Table 2; Fig. 5). Landsat data have been used to demonstrate greening in the Arctic; that is, 29.4% of Canada and Alaska demonstrated positive greening (Ju and Masek, 2016). The authors generated a peak-summer Landsat composite from 1984 to

2012 that illustrates precise changes in greening and browning (http://www.nasa.gov/sites/default/files/thumbnails/image/agstill.3975legend.jpg). Whereas the tendency for greening is predominant, the trends are extremely variable across latitude and longitude, with some significant browning in the interior of Alaska and central Canada. The results of our study are consistent with the findings of Ju and Masek (2016), where there is a greening trend for the CBAWO and no clear trend for the ARW. Further, a general trend of greening has been reported by Fraser et al. (2011) for four national parks in Canada at various locations within the Arctic (albeit all south of the CBAWO). Specifically, the authors discovered an increase in NDVI specific to the shrub/graminoid vegetation class (similar to a mesic vegetation type); where the increase in greenness occurred in areas of already favorable growing conditions. The authors observed consistent patterns of greening (i.e., 6.1–25.5%) that were attributed to increased fractional shrub and other vegetation cover that was associated with positive temperature trends (similar to our observations at the CBAWO).

Epstein et al. (2016) demonstrated greening to be predominant on the North Slope of Alaska, the tundra of southern Canada, and in central and eastern Siberia, whereas browning tends to be prevalent in western Alaska, western Siberia, and the Canadian High Arctic. This result for the Canadian High Arctic may be a function of the scale of observation (i.e., AVHRR), given we observed greening at intermediate spatial scales (i.e., Landsat) for the CBAWO. Analyses of different scales will provide different results, or at least potentially mask trends that are more gradual. For example, Fraser et al. (2011) observed that gradual greening trends observed with Landsat data were not apparent at coarser scales (i.e., 3 km NDVI derived from AVHRR data), likely attributable to spatial averaging, indicating the importance of higher spatial resolution data to characterize vegetation change at regional or local scales. This emphasizes the importance of examining different locations within the circumpolar region at multiple scales in concert with field observations.

The static trend observed at the Low Arctic site (i.e., ARW) was similar to a study conducted by Pattison et al. (2015). The authors combined plot-level trends in species composition with fine and coarse spatial resolution NDVI trends in Alaska from 1984 to 2009. At the plot level, none of the five vegetation types that were measured appeared to change in species composition; and in conjunction, the Landsat time series also demonstrated no change in NDVI. Although results in the ARW and the results published by Pattison et al. (2015) demonstrate no significant greening at these Low Arctic

sites, not all studies have reported similar results. Fraser et al. (2011) found that all Low Arctic study sites (on the East and West side of the Low Arctic) above treeline were significantly greening using Landsat time series over a 17- to 25-year period. Similarly, Raynolds et al. (2013) observed a significant increase in greenness on the North Slope of Alaska (from 1985 to 2007) using Landsat data, and Epstein et al. (2012) found a 19.8% increase in aboveground biomass from 1982 to 2010 using AVHRR data based on vegetation subzones. The area of most notable change was documented in the Low Arctic. Again, this variability observed for the Low Arctic can be attributed to the location of specific studies as well as the scale of observation. Hence, we need to be careful to consider spatial and temporal scales when generalizing trends of greening and/or browning for any given location, particularly at broad scales.

Climate Variables—Temperature, Precipitation, and Growing Season Length

The inherent change in NDVI across the Canadian Arctic and for specific vegetation types has been linked to July temperatures and GSL. In some areas of the Arctic, where temperatures tend to be increasing, growing seasons tend to lengthen, leading to enhanced greening (Tucker et al., 2001; Cooper et al., 2011; Bieniek et al., 2015; Moffat et al., 2016). Gamon et al. (2013) agreed that GDD, local environmental conditions, and temperature are primary factors determining arctic vegetation productivity. Further, the SWI has also been linked to increases in NDVI using coarse resolution satellite data of the circumpolar Arctic (Jia et al., 2009; Bhatt et al., 2013). Bhatt et al. (2013) also stated that from 1982 to 2011, at a Pan-Arctic scale, summer (May–August) land surface temperatures and NDVI increased in concert with an increase in open water. Raynolds et al. (2008) found that the regression of NDVI as a function of SWI showed a highly significant positive relationship, where a 5 °C increase in the SWI corresponded to a 0.07 increase in NDVI (i.e., corresponding to increases in growing season temperatures) over the entire Arctic. Our results support the close relationship between significant increases in temperature, GSL, and NDVI (Tables 2 and 3; Figs. 5, 6, and 7).

The contrasting climate trends observed at the two study sites (Figs. 6 and 7) support the increase in NDVI at the CBAWO compared to the lack of an NDVI trend at the ARW (Fig. 5). ACIA (2004) and IPCC (2013) each stated that the mean annual and winter temperatures along the west coast of the Arctic are generally higher than those at latitudes inland or on the east coast

because of Arctic, Pacific, and North Atlantic Oscillations. For example, the North Atlantic Oscillation demonstrates a trend favoring the positive phase over the past four decades resulting in colder temperatures in the east (IPCC, 2013). In some studies, winter temperatures and snowmelt timing have been found to correlate with vegetation growth the following summer (Myers-Smith et al., 2011). The results reported here suggest that compared to the ARW (an eastern Low Arctic site), there was proportionately more greening at the CBAWO (a western High Arctic site), which can be attributed, in part, to higher summer temperatures (Fig. 6, part b) and an increased GSL (Fig. 7, part b). Results like these can be applied to validate and project the impacts of a changing climate as predicted by GCMs, and can be used to examine where vegetation changes can be anticipated over the coming decades. However, although greening may be occurring in large portions of the Arctic (indicating increasing productivity of arctic biomass), evidence suggests that this greening will not offset the release of organic carbon due to decomposition, combustion, and hydrologic export (Abbott et al., 2016). Given this positive feedback scenario, it is expected that the Arctic will become a carbon source to the atmosphere, regardless of the warming scenario. Hence, not only is monitoring of the vegetation response important, as examined in this study, we need to better model carbon flux within and between vegetation types that are responding differently across the Arctic.

CONCLUSION

Monitoring vegetation change in the Arctic is an important process for examining the variable impacts of a warming climate. Due to the vast expanse of the largely uninhabited Arctic, remote sensing techniques must be employed at various spatial and temporal scales to examine and quantify this change. This has become somewhat routine at circumpolar scales using coarse resolution satellite data. In this study, mapping and analyzing heterogeneous arctic landscapes at intermediate and high spatial resolutions was beneficial for characterizing how specific vegetation types (defined along a moisture gradient) have (or have not) changed over time in the context of climate change. NDVI time series were derived using intermediate spatial resolution data (i.e., Landsat) at Low and High Arctic study sites. The NDVI time series for both sites were coupled with high resolution land-cover classifications in order to identify specific vegetation types and quantify their response to climate. The results for the CBAWO (1985–2015) indicated a significant positive trend in the mesic tundra and polar semi-desert vegetation types, whereas no sig-

nificant trends were observed in the ARW. Temperature, precipitation and GSL were analyzed in an attempt to identify the primary environmental variables driving the increases in NDVI at the CBAWO. The mean July temperature trend increases significantly at the CBAWO (based on climate data from Mould Bay). Similarly, there is a significant positive trend in GSL for the CBAWO. It therefore seems apparent that there is a link between changes in NDVI, mean July temperature, and GSL at the CBAWO (i.e., High Arctic). Meanwhile, no significant trends in NDVI or any of the climate variables examined were observed for the ARW. Whereas increasing temperatures and GSL may be driving enhanced productivity at the CBAWO, the climatic trends at the ARW may be largely driven by climate oscillations (i.e., Arctic, Pacific, and North Atlantic Oscillations), thereby dampening the potential change in the eastern Low Arctic.

REFERENCES CITED

Abbott, B. W., Jones, J. B., Schuur, E. A. G., Chapin, F. S., III, Bowden, W. B., Bret-Harte, M. S., Epstein, H. E., Flannigan, M. D., Harms, T. K., Hollingsworth, T. N., Mack, M. C., McGuire, A. D., Natali, S. M., Rocha, A. V., Tank, S. E., Turetsky, M. R., Vonk, J. E., Wickland, K. P., Aiken, G. R., Alexander, H. D., Amon, R. M. W., Benscoter, B. W., Bergeron, Y., Bishop, K., Blarquez, O., Bond-Lamberty, B., Breen, A. L., Buffam, I., Cai, Y., Carcaillet, C., Carey, S. K., Chen, J. M., Chen, H.Y. H., Christensen, T. R., Cooper, L. W., Cornelissen, J. H. C., de Groot, W. J., DeLuca, T. H., Dorrepaal, E., Fetcher, N., Finlay, J. C., Forbes, B. C., French, N. H. F., Gauthier, S., Girardin, M. P., Goetz, S. J., Goldammer, J. G., Gough, L., Grogan, P., Guo,

L., Higuera, P. E., Hinzman, L., Hu, F. S., Hugelius, G., Jafarov, E. E., Jandt, R., Johnstone, J. F., Karlsson, J., Kasischke, E. S., Kattner, G., Kelly, R., Keuper, F., Kling, G. W., Kortelainen, P., Kouki, J., Kuhry, P., Laudon, H., Laurion, I., Macdonald, R. W., Mann, P. J., Martikainen, P. J., McClelland, J. W., Molau, U., Oberbauer, S. F., Olefeldt, D., Paré, D., Parisien, M.-A., Payette, S., Peng, C., Pokrovsky, O. S., Rastetter, E. B., Raymond, P. A., Raynolds, M. K., Rein, G., Reynolds, J. F., Robards, M., Rogers, B. M., Schädel, C., Schaefer, K., Schmidt, I. K., Shvidenko, A., Sky, J., Spencer, R. G. M., Starr, G., Striegl, R. G., Teisserenc, R., Tranvik, L. J., Virtanen, T., Welker, J. M., and Zimov, S., 2016: Biomass offsets little or none of permafrost carbon release from soils, streams, and wildfire: an expert assessment. *Environmental Research Letters*, 11: 034014; doi: http://dx.doi.org/10.1088/1748-9326/11/3/034014.

ACIA [Arctic Climate Impact Assessment], 2004: *Arctic Climate Impact Assessment—Scientific Report*. Cambridge, U.K.: Cambridge University Press.

AMAP, 2011: *Snow, Water, Ice and Permafrost in the Arctic (SWIP A): Climate Change and the Cryosphere*. Oslo, Norway: Arctic Monitoring and Assessment Program (AMAP), xii–538 pp.

Atkinson, D. M., and Treitz, P., 2012: Arctic ecological classifications derived from vegetation community and satellite spectral data. *Remote Sensing*, 4(12): 3948–3971.

Atkinson, D. M., and Treitz, P., 2013: Modeling biophysical variables across an Arctic latitudinal gradient using high spatial resolution remote sensing data. *Arctic, Antarctic, and Alpine Research*, 45(2): 161–178.

Barber, D. G., Lukovich, J. V., Keogak, J., Baryluk, S., Fortier, L., and Henry, G. H. R., 2008: The changing climate of the Arctic. *Arctic*, 61(Suppl. 1): 7–26.

Beck, P., and Goetz, S., 2011: Satellite observations of high northern latitude vegetation productivity changes between 1982 and 2008: ecological variability and regional differences. *Environmental Research Letters*, 6: 045501; doi: http://dx.doi.org/10.1088/1748-9326/6/4/045501.

Bhatt, U. S., Walker, D. A., Raynolds, M. K., Bieniek, P. A., Epstein, H. E., Comiso, J. C., Pinzon, J. E., Compton T. J., and Polyakov, I. V., 2013: Recent declines in warming and vegetation greening trends over pan-arctic tundra. *Remote Sensing,* 5: 4229–4254.

Bieniek, P. A., Bhatt, U. S., Walker, D. A., Raynolds, M. K., Comiso, J. C., Epstein, H. E., Pinzon, J. E., Tucker, C. J., Thoman, R. L., Tran, H., Mölders, N., Steele, M., Zhang, J., and Ermold, W., 2015: Climate drivers linked to changing seasonality of Alaska coastal tundra vegetation productivity. *Earth Interactions*, 19(19): 1–29.

Bjerke, J. W., Karlsen, S. R., Hogda, K. A., Malnes, E., Jepsen, J. U., Lovibond, S., Vikhamar-Schuler, D., and Tømmervik, H., 2014: Record-low primary productivity and high plant damage in the Nordic Arctic Region in 2012 caused by multiple weather events and pest outbreaks. *Environmental Research Letters*. 9: 084006; doi: http://dx.doi.org/10.1088/1748-9326/9/8/084006.

Boisvert, L. N., and Stroeve, J. C., 2015: The Arctic is becoming warmer and wetter as revealed by the Atmospheric Infrared Sounder. *Geophysical Research Letters*, 42: 4439–4446.

Bratsch, S. N., Epstein, H. E., Buchhorn, M., and Walker, D. A., 2016: Differentiating among four Arctic tundra plant communities at Ivotuk, Alaska using field spectroscopy. *Remote Sensing*, 8(1): 51; doi://dx.doi.org/10.3390/rs8010051.

Brown, M. E., Pinzón, J. E., Didan, K., Morisette, J. T., and Tucker, C. J., 2006: Evaluation of the consistency of Long-term NDVI time series derived from AVHRR, SPOT-vegetation, SeaWiFS, MODIS, and Landsat ETM+ sensors. *IEEE Transactions on Geoscience and Remote Sensing*, 44(7): 1787–1793.

Cameron, E. A., and Lantz, T. C., 2016: Drivers of tall shrub proliferation adjacent to the Dempster Highway, Northwest Territories, Canada. *Environmental Research Letters*, 11(4): 1–11.

Carter, T., 1998: Changes in the thermal growing season in Nordic countries during the past century and prospects for the future. *Agricultural and Food Science in Finland,* 7: 161–179.

CAVM Team, 2003: Circumpolar Arctic Vegetation Map. Anchorage, Alaska: U.S. Fish and Wildlife Service, Conservation of Arctic Flora and Fauna (CAFF) Map No. 1, (1:7,500,000 scale).

Chen, A., Chen, W., Leblanc, S., and Henry, G., 2010: Digital photograph analysis for measuring percent plant cover in the Arctic. *Arctic*, 63(3): 315–326.

Collingwood, A., Treitz, P., Charbonneau, F., and Atkinson, D., 2014: Artificial neural network modeling of High Arctic phytomass using synthetic aperture radar and multispectral data. *Remote Sensing*, 6(3): 2134–2153.

Cooper, E. J., Dullinger, S., and Semenchuk, P., 2011: Late snowmelt delays plant development and results in lower reproductive success in the High Arctic. *Plant Science*, 180(1): 157–167.

Davidson, S. J., Santos, M. J., Sloan, V. L., Wattts, J. D., Phoenix, G. K., Oechel, W. C., and Zona, D., 2016: Mapping Arctic tundra vegetation communities using field spectroscopy and multispectral satellite data in North Alaska, USA. *Remote Sensing*, 8(12): 978; doi://dx.doi.org/10.3390/rs8120978.

Edlund, S. A., 1993: The distribution of plant communities on Melville Island, Arctic Canada. *In* Christie, R. L., and McMillan, J. (eds.); *The Geology of Melville Island, Arctic Canada*. Geological Survey of Canada Bulletin 450: 247–255.

Elmendorf, S. C., Henry, G. H. R., Hollister, R. D., Björk, R. G., Bjorkman, A. D., Callaghan, T. V., Collier, L. S., Cooper, E. J., Cornelissen, J. H. C., Day, T. A, Fosaa, A. M., Gould, W. A., Grétarsdóttir, J., Harte, J., Hermanutz, L., Hik, D. S., Hofgaard, A., Jarrad, F., Jónsdóttir, I. S., Keuper, F., Klanderud, K., Klein, J. A., Koh, S., Kudo, G., Lang, S., Loewen, V., May, J. L., Mercado, J., Michelsen, A., Molau, U., Myers-Smith, I. H., Oberbauer, S. F., Pieper, S., Post, E., Rixen, C., Robinson, C. H., Martin Schmidt, N., Shaver, G. R., Stenström, A., Tolvanen, A., Totland, Ø., Troxler, T., Wahren, C.-H., Webber, P. J., Welker, J. M., and Wookey, P. A., 2012: Global assessment of experimental climate warming on tundra vegetation: heterogeneity over space and time. *Ecology Letters*, 15: 164–175.

Environment and Climate Change Canada, 2015: Homogenized temperature and precipitation. http://www.ec.gc.ca/dccha-ahccd/. Accessed 21 April 2016.

Epstein, H. E., Raynolds, M. K., Walker, D. A., Bhatt, U. S., Tucker, C. J., and Pinzon, J. E., 2012: Dynamics of aboveground phytomass of the circumpolar Arctic tundra during the past three decades. *Environmental Research Letters*, 7: 1–12.

Epstein, H. E., Bhatt, U. S., Raynolds, M. K., Walker, D. A., Bieniek, P. A., Tucker, C. J., Pinzon, J., Myers-Smith, I. H., Forbes, B. C., Macias-Fauria, M., Boelman, N. T., and Sweet, S. K., 2015: Tundra greenness. *In* Jeffries, M. O., Richter-Menge, J., and Overland, J. E. (eds.), Arctic Report Card: Update for 2015. NOAA, Silver Spring, Maryland. http://www.arctic.noaa.gov/Report-Card/. Accessed 12 April 2017.

Epstein, H. E., Bhatt, U. S., Raynolds, M. K., Walker, D. A., Forbes, B. C., Macias-Fauria, M., Loranty, M., Phoenix, G., and Bjerke, J., 2016: Tundra greenness. *In* Richter-Menge, J., Overland, J. E., and Mathis, J. T. (eds.), Arctic Report Card: Update for 2016. NOAA, Silver Spring, Maryland. http://www.arctic.noaa.gov/Report-Card/. Accessed 12 April 2017.

Fensholt, R., and Proud, S. R., 2012: Evaluation of earth observation based global long term vegetation trends—Comparing GIMMS and MODIS Global NDVI Time Series. *Remote Sensing of Environment,* 119: 131–147.

Fitzpatrck-Lins, K., 1981: Comparison of sampling procedures and data analysis for a land-use and land-cover map. *Photogrammetric Engineering and Remote Sensing*, 47(3): 343–351.

Forbes, B. C., Fauria, M. M., and Zetterberg, P., 2010: Russian Arctic warming and 'greening' are closely tracked by tundra shrub willows. *Global Change Biology*, 16: 1542–1554.

Forkel, M., Carvalhais, N., Verbesselt, J., Mahecha, M., Neigh, C., and Reichstein, M., 2013: Trend change detection in NDVI time series: effects of inter-annual variability and methodology. *Remote Sensing*, 5(5): 2113–2144.

Fraser, R. H., Olthof, I., Carrière, M., Deschamps, A., and Pouliot, D., 2011: Detecting long-term changes to vegetation in northern Canada using the Landsat satellite image archive. *Environmental Research Letters*, 6: 045502; doi: http://dx.doi.org/10.1088/1748-9326/6/4/045502.

Fraser, R. H., Lantz, T. C., Olthof, I., Kokelj, S. V., and Sims, R. A., 2014: Warming-induced shrub expansion and lichen decline in the Western Canadian Arctic. *Ecosystems*, 17: 1151–1168.

Førland, E., Skaugen, T., and Benestad, R., 2004: Variations in thermal growing, heating, and freezing indices in the Nordic Arctic, 1900–2050. *Arctic, Antarctic, and Alpine Research,* 36: 347–356.

Gamon, J. A., Huemmrich, K. F., Stone, R. S., and Tweedie, C. E., 2013: Spatial and temporal variation in primary productivity (NDVI) of coastal Alaskan tundra: decreased vegetation growth following earlier snowmelt. *Remote Sensing of Environment*, 129: 144–153.

Gregory, F. M., 2011: Biophysical remote sensing and terrestrial CO_2 exchange at Cape Bounty, Melville Island. MSc thesis, Queen's University, Kingston, Ontario.

Guay, K. C., Beck, P. A., Berner, L. T., Goetz, S. J., Baccini, A., and Buermann, W., 2014: Vegetation productivity patterns at high northern latitudes: a multi-sensor satellite data assessment. *Global Change Biology*, 20: 3147–3158.

Hinzman, L. D., Bettez, N. D., Bolton, W. R., Chapin, F. S., Dyurgerov, M. B., Fastie, C. L., Griffith, B., Hollister, R. D., Hope, A., Huntington, H. P., Jensen, A. M., Jia, G. J., Jorgenson, T., Kane, D. L., Klein, D. R., Kofinas, G., Lynch, A. H., Lloyd, A. H., McGuire, D. A., Nelson, F., Oechel, W. C., Osterkamp, T. E., Racine, C. H., Romanovsky, C. E., Stone, R. S., Stow, D. A., Strum, M., Tweedie, C. E., Vourlitis, G. L., Walker, M. D., Walker, D. A., Webber, P. J., Welker, J. M., Winker, K. S., and Yoshikawa, K., 2005: Evidence and implications of recent climate change in northern Alaska and other Arctic regions. *Climatic Change*, 72(3): 251–298.

Hollister, R. D., Webber, P. J., and Tweedie, C. E., 2005: The response of Alaskan arctic tundra to experimental warming: differences between short- and long-term responses. *Global Change Biology*, 11, 525–536.

Hope, A. S., Kimball, J. S., and Stow, D. A., 1993: The relationship between tussock tundra spectral reflectance properties and biomass and vegetation composition. *International Journal of Remote Sensing*, 14: 1861–1874.

Huemmrich, K. F., Gamon, J. A., Tweedie, C. E., Oberbauer, S. F., Kinoshita, G., Houston, S., Kuchy, A., Hollister, R. D., Kwon, H., Mano, M., Harazono, Y., Webber, P. J., and Oechel, W. C., 2010: Remote sensing of tundra gross ecosystem productivity and light use efficiency under varying temperature and moisture conditions. *Remote Sensing of Environment*, 114(3): 481–489.

IPCC, 2013: Summary for policymakers. *In* Stocker, T. F., Qin, D., Plattner, G.-K., Tignor, M., Allen, S. K., Boschung, J., Nauels, A., Xia, Y., Bex V., and Midgley, P. M. (eds.), *Climate Change 2013: The Physical Science Basis. Contribution of Working Group I to the Fifth Assessment Report of the Intergovernmental Panel on Climate Change*. Cambridge and New York: Cambridge University Press.

Jacobs, J. D., Headley, A. N., Maus, L. A, Mode, W. N., and Simms, E. L., 1997: Climate and vegetation of the interior lowlands of southcentral Baffin Island: long-term stability at the low Arctic limit. *Arctic*, 50(2): 167–177.

Jensen, J. R., 2005: *Introductory Digital Image Processing a Remote Sensing Perspective*. 3rd edition. Upper Saddle River, New Jersey: Pearson Education, Inc.

Jia, G. J., and Epstein, H. E., 2003: Greening of Arctic Alaska, 1981–2001. *Geophysical Research Letters*, 30(20): 3–6.

Jia, G. J., Epstein, H. E., and Walker, D. A., 2009: Vegetation greening in the Canadian Arctic related to decadal warming. *Journal of Environmental Monitoring*, 11: 2231–2238.

Johansen, B., and Tømmervik, H., 2014: The relationship between phytomass, NDVI and vegetation communities on Svalbard. *International Journal of Applied Earth Observation and Geoinformation*, 27: 20–30.

Ju, J., and Masek, J. G., 2016: The vegetation greenness trend in Canada and US Alaska from 1984–2012 Landsat data. *Remote Sensing of Environment*, 176: 1–16.

Kattsov, V. M., and Walsh, J. E., 2000: Twentieth-century trends of Arctic precipitation from observational data and a climate model simulation. *Journal of Climate*, 13(8): 1362–1370.

Laidler, G., Treitz, P., and Atkinson, D., 2008: Remote sensing of Arctic vegetation: relations between the NDVI, spatial resolution, and vegetation cover on Boothia Peninsula, Nunavut. *Arctic,* 61(1): 1–13.

Lamoureux, S. (unpublished data): 2003–2015 climate data, west station, Cape Bounty, Nunavut. Accessed February 2015.

Lantz, T. C., Gergel, S. E., and Kokelj, S. V., 2010: Spatial heterogeneity in the shrub tundra ecotone in the Mackenzie Delta region, Northwest Territories: implications for Arctic environmental change. *Ecosystems*, 13(2): 194–204.

Leblanc, A. M., Short, N., Oldenborger, G. A., Mathon-Dufour, V., and Allard, M., 2012: Geophysical investigation and InSAR mapping of permafrost and ground movement at the Iqaluit airport. *In* Doré, G., and Morse, B. (eds), *Cold Regions Engineering 2012, Sustainable Infrastructure Development in a Changing Cold Environment*. Quebec: American Society of Civil Engineers, 644–654.

Liu, N., and Treitz, P., 2016: Modelling high arctic percent vegetation cover using field digital images and high resolution satellite data. *International Journal of Applied Earth Observation*, 52: 445–456.

Miles, V. V., and Esau, I., 2016: Spatial heterogeneity of greening and browning between and within bioclimatic zones in northern West Siberia. *Environmental Research Letters*, 11: 115002; doi: http://dx.doi.org/10.1088/1748-9326/11/11/115002.

Moffat, N. D., Lantz, T. C., Fraser, R. H., and Olthof, I., 2016: Recent vegetation change (1980–2013) in the tundra ecosystems of the Tuktoyaktuk Coastlands, NWT, Canada. *Arctic, Antarctic, and Alpine Research*, 48(3): 581–597.

Molau, U., and Mølgaard, P. (eds.), 1996: *International Tundra Experiment (ITEX) Manual*. Second Edition. Copenhagen, Denmark: Danish Polar Centre.

Myers-Smith, I. H., Forbes, B. C., Wilmking, M., Hallinger, M., Lantz, T., Blok, D., Tape, K. D., Macias-Fauria, M., Sass-Klaassen, U., Levesque, E., Boudreau, S., Ropars, P., Hermanutz, L., Trant, A., Collier, L. S., Weijers, S., Rozema, J., Payback, S. A., Schmidt, N. M., Schaepman-Strub, G., Wipf, S., Rixen, C., Menard, C. B., Venn, S., Goetz, S., Audreu-Hayles, L., Elmendorf, S., Ravolainen, V., Welker, J., Grogan, P., Epstein, H. E., and Hik, D. S., 2011: Shrub expansion in tundra ecosystems: dynamics, impacts and research priorities. *Environmental Research Letters*, 6(4): 1–15.

Myers-Smith, I. H., Elmendorf, S. C., Beck, P. S. A., Wilmking, M., Hallinger, M., Blok, D., Tape, K. D., Rayback, S. A., Macias-Fauria, M., Forbes, B. C., Speed, J. D. M., Boulangier-Lapointe, N., Rixen, C., Lévesque, E., Martin Schmidt, N., Baittinger, C., Trant, A. J., Hermanutz, L., Siegwart Collier, L., Dawes, M. A., Lantz, T. C., Weijers, S., Haalfdan Jørgensen, R., Buchwal, A., Bura, A., Naito, A. T., Ravolainen, V., Schaepman-Strub, G., Wheeler, J. A., Wipf, S., Guay, K. C., Hik, D. S., and Vellend, M., 2015: Climate sensitivity of shrub growth across the tundra biome. *Nature Climate Change*, 5: 887–892.

National Aeronautics and Space Administration (NASA), 2017: NASA Studies Details of a Greening Arctic. https://www.nasa.gov/sites/default/files/thumbnails/image/agstill.3975legend.jpg. Accessed 9 June 2016.

Natural Resources Canada, 2012: Surficial Geology, Iqaluit, Nunavut. http://geogratis.gc.ca/api/en/nrcan-rncan/ess-sst/2744fedb-5213-5d4b-968e-5982c8497a38.html?pk_campaign=recentItem. Accessed December 2015.

Natural Resources Canada, 2015: Hydrological Layers. http://geogratis.gc.ca/site/eng/extraction. Accessed November 2015.

Necsoiu, M., Longepe, N., and Hooper, D., 2013: A new methodology to monitor soil moisture over a complex Arctic environment, Kobuk River valley, Alaska. *Remote Sensing Letters,* 4(3): 251–260.

Obradovic, M. M., and Sklash, M. G., 1986: An isotopic and geochemical study of snowmelt runoff in a small Arctic watershed. *Hydrological Processes*, 1: 15–30.

Olthof, I., and Fraser, R., 2014: Detecting landscape changes in high latitude environments using Landsat trend analysis: 2. Classification. *Remote Sensing,* 6: 11558–11578.

Olthof, I., and Latifovic, R., 2007: Short-term response of arctic vegetation NDVI to temperature anomalies. *International Journal of Remote Sensing,* 28(21): 4823–4840.

Ostendorf, B., and Reynolds, J., 1998: A model of Arctic tundra vegetation derived from topographic gradients. *Landscape Ecology*, 13: 187–201.

Pattison, R. R., Jorgenson, J. C., Raynolds, M. K., and Welker, J. M., 2015: Trends in NDVI and tundra community composition in the Arctic of NE Alaska between 1984 and 2009. *Ecosystems*, 18: 707–719.

Pearson, R. G., Phillips, S. J., Loranty, M. M., Beck, P. S. A., Damoulas, T., Knight, S. J., and Goetz, S. J., 2013: Shifts in Arctic vegetation and associated feedbacks under climate change. *Nature Climate Change*, 3(7): 673–677.

Phoenix, G. K., and Bjerke, J. W., 2016: Arctic browning: extreme events and trends reversing arctic greening. *Global Change Biology*, 22: 2960–2962.

Pinzon, J. E., and Tucker, C. J., 2014: A non-stationary 1981–2012 AVHRR NDVI3g time series. *Remote Sensing*, 6(8): 6929–6960.

Raynolds, M., Comiso, J., Walker, D., and Verbyla, D., 2008: Relationship between satellite-derived land surface temperatures, Arctic vegetation types, and NDVI. *Remote Sensing of Environment*, 112(4): 1884–1894.

Raynolds, M. K., Walker, D. A., Epstein, H. E., Pinzon, J. E., and Tucker, C. J., 2012: A new estimate of tundra-biome phytomass from trans-Arctic field data and AVHRR NDVI. *Remote Sensing Letters*, 3, 403–411.

Raynolds, M. K., Walker, D. A., Verbyla, D., and Munger, C. A., 2013: Patterns of change within a tundra landscape: 22-year Landsat NDVI trends in an area of the northern foothills of the Brooks Range, Alaska. *Arctic, Antarctic, and Alpine Research*, 45(2): 249–260.

Rudy, A., Lamoureux, S., Treitz, P., and Collingwood, A., 2013: Identifying permafrost slope disturbance using multi-temporal optical satellite images and change detection techniques. *Colds Regions Science and Technology*, 88: 37–49.

Sedden, A. W. R., Macias-Fauria, M., Long, P. R., Benz, D., and Willis, K. J., 2016: Sensitivity of global terrestrial ecosystems to climate variability. *Nature*, 531: 229–232; doi: http://dx.doi.org/10.1038/nature16986.

Skaugen, T. E., and Tveito, O. E., 2004: Growing-season and degree-day scenario in Norway for 2021–2050. *Climate Research,* 26: 221–232.

Stow, D., Daeschner, S., Hope, A., Douglas, D., Petersen, A., Myneni, R., Zhou, L., and Oechel, W., 2003: Variability of the seasonally integrated normalized difference vegetation index across the North Slope of Alaska in the 1990s. *International Journal of Remote Sensing*, 24(5): 1111–1117.

Stow, D. A., Hope, A., McGuire, D., Verbyla, D., Gamon, J., Huemmrich, F., Houston, S., Racine, C., Sturm, M., Tape, K., Hinzman, L., Yoshikawa, K., Tweedie, C. Noyle, B., Silapaswan, C., Douglas, D., Griffith, B., Jia, G., Epstein, H., Walker, D., Daeschner, S., Petersen, A. Zhou, L., and Myneni, R., 2004: Remote sensing of vegetation and land-cover change in Arctic tundra ecosystems. *Remote Sensing of Environment*, 89: 281–308.

Thomas, V., Treitz, P., Jelinski, D., Miller, J., Lafleur, P., and McCaughey, H., 2002: Image classification of northern peatland complex using spectral and plant community data. *Remote Sensing of Environment*, 84: 83–99.

Tingley, M. P., and Huybers, P., 2013: Recent temperature extremes at high northern latitudes unprecedented in the past 600 years. *Nature*, 496: 201–205.

Tucker, C. J., Slayback, D. A., Pinzon, J. E., Ranga, S. O. L., and Taylor, M. G., 2001: Higher northern latitude normalized difference vegetation index and growing season trends from 1982 to 1999. *International Journal of Biometeorology*, 7: 184–190.

Urban, M., Forkel, M., Eberle, J., Hüttich, C., Schmullius, C., and Herold, M., 2014: Pan-Arctic climate and land cover trends derived from multi-variate and multi-scale analyses (1981–2012). *Remote Sensing*, 6: 2296–2316.

USGS, 2015: Landsat Imagery. http://glovis.usgs.gov/. Accessed October 2015.

Walker, D. A., Raynolds, M. K., Daniëls, F. J. A., Einarsson, E., Elvebakk, A., Gould, W. A., Katenin, A. E., Kholodo, S. S., Markon, C. J., Melnikov, E. S., Moskalenko, N. G., Talbot, S. S., Yurtsev, B. A., and other members of the CAVM Team, 2005: The Circumpolar Arctic Vegetation Map. *Journal of Vegetation Science*, 16(3): 267–282.

Walker, M. D., Wahren, H. C., Hollister R. D., Henry. G. H., Ahlquist. L. E., Alatalo. J. M., Bret-Harte, M. S., Calef, M. P., Callaghan, T. V., Carroll, A. B., Epstein, H. E., Jonsdottir, I. S., Klein, J. A., Magnusson, B., Molau, U., Oberbauer, S. F., Rewa, S. P., Robinson, C. H., Shaver, G. R., Suding, K. N., Thompson, C. C., Tolvanen, A., Totland, O., Turner, P. L., Tweedie, C. E., Webber, P. J., and Wookey, P. A., 2006: Plant community responses to experimental warming across the tundra biome. *PNAS*, 103(5): 1342–1346.

Walker, D. A., Leibman, M. O., Epstein, H. E., Forbes, B. C., Bhatt, U. S., Raynolds, M. K., Comiso, J. C., Gubarkov, A. A., Khomutov, A. V., Jia, G. J., Kaarlejärvi, E., Kaplan, J. O., Kumpula, T., Kuss, P., Matyshak1, G., Moskalenko, N. G., Orekhov, P., Romanovsky, V. E., Ukraientseva, N. G., and Yu, Q., 2009: Spatial and temporal patterns of greenness on the Yamal Peninsula, Russia: interactions of ecological and social factors affecting the Arctic normalized difference vegetation index. *Environmental Research Letters*, 4(4):045004; doi: http://dx.doi.org/10.1088/1748-9326/4/4/045004.

Weijers, S., Wagner-Cremer, F., Sass-Klaassen, U., Broekman, R., and Rozema, J., 2013: Reconstructing High Arctic growing season intensity from shoot length growth of a dwarf shrub. *The Holocene*, 23(5): 721–731.

Welker, J. M., Fahnestock, J. T., Sullivan, P. F., and Chimner, R. A., 2005: Leaf mineral nutrition of Arctic plants in response to warming and deeper snow in northern Alaska. *Oikos,* 109(1): 167–177.

Xu, L., Myneni, R. B., Chapin, P. S., III, Callaghan, T. V., Pinzon, J. E., Tucker, C. J., Zhu, Z., Bi, J., Ciais, P., Tømmervik, H., Euskirchen, E. S., Forbes, B. C. Piao, S. L., Anderson, B. T., Ganguly, S., Nemani, R. R., Goetz, S. J., Beck, P. S. A., Bunn, A. G., Cao, C., and Stroeve, J. C., 2013: Temperature and vegetation seasonality diminishment over northern lands. *Nature Climate Change*, 3: 581–586.

Yin, H., Udelhoven, T., Fensholt, R., Pflugmacher, D., and Hostert, P., 2012: How normalized difference vegetation index (NDVI) trends from Advanced Very High Resolution Radiometer (AVHRR) and système probatoire d'observation de la terre VEGETATION (SPOT VGT) time series differ in agricultural areas: an Inner Mongolian case study. *Remote Sensing*, 4(12): 3364–3389.

Zeng, H., Jia, G., and Epstein, H., 2011: Recent changes in phenology over the northern high latitudes detected from multi-satellite data. *Environmental Research Letters*, 6: 1–11.